Preprints (www.preprints.org) | NOT PEER-REVIEWED | Posted: 5 June 2020 doi:10.20944/preprints202006.0053.v1

Row Action Algebraic Reconstruction Techniques Implementation in Graphic Cards using SCILAB

(Benchmark in Medical Imaging, Seismic Imaging and Walnut Imaging)

M. Ilyas[1], A.D. Garnadi[2,*], M.T. Julianto[3],S. Nurdiati[4]

[1]School of Mathematical and Physical Sciences, The University of Newcastle, Australia; muhammad.ilyas@newcatle.edu.au

[2]Department of Mathematics, Bogor Agricultural University, Bogor, Indonesia; agah.garnadi@gmail.com

[2]Department of Mathematics, Bogor Agricultural University, Bogor, Indonesia; mtjulianto@gmail.com

[2]Department of Mathematics, Bogor Agricultural University, Bogor, Indonesia; s.nurdiati@gmail.com

*Correspondence:agah.garnadi@gmail.com ; Tel.: +62-251-8625-276

Abstract: In this article we present a SCILAB implementation of algebraic iterative reconstruction methods for discretisation of inverse problems in imaging. These so-called row action methods rely on semi-convergence for achieving the necessary regularisation of the problem. We implement this method using SCILAB and provide a few simplified test problems: medical tomography, seismic tomography and walnut tomography.Numerical results show the capability of this method for the original and perturbed right-hand side vector.

Keywords: Algebraic iterative reconstruction; ART methods; Row-action methods; Graphics Cards;Tomographic imaging; Medical imaging; Seismic Imaging; Walnut Imaging.

---

1. Introduction

Iterative reconstruction method for computing solutions to discretization of inverse problems have been used for decades in medical imaging, geophysics, material science and many other disciplines that involve 2D and 3D imaging [1]. This article presents algebraic reconstruction techniques to solve large linear systems of the form

$$A\boldsymbol{x} \cong \mathbf{b}, A \in \mathbb{R}^{m\times n}$$

used in tomography and many other inverse problems. We assume that the elements of matrix A are nonnegative and contains non zero rows or columns.

There are no restriction on the dimensions.We can write the system of linear equations with m equations with n unknown variables:

$$\mathbf{a}_i^T\mathbf{x} = b_i, \qquad i = 1, 2, \dots, m$$

where$\mathbf{a}_i$ and $\mathbf{x}$are column vectors. Observe that the$m$ equation are hyperplanesin $\mathbb{R}^n$, an$n$-dimensional Euclidean space.

2. Algebraic Reconstruction Techniques

This section may be divided by subheadings. It should provide a concise and precise description of the experimental results, their interpretation as well as the experimental conclusions that can bedrawn.

Algebraic Reconstruction Technique (ART) is one of the method used in commercial machine.The earliest row action ART iterative method proposed by S. Kaczmarz in 1937 in his paper "*Angenäherte auflösung von systemen linearer gleichungen*". [2]

Preprints (www.preprints.org) | NOT PEER-REVIEWED | Posted: 5 June 2020 doi:10.20944/preprints202006.0053.v1

The core of ART method is the row-action method that treat the equation one at a time during the iterations. ART method find orthogonal projection $\mathbf{x}_{k+1}$ from $\mathbf{x}_k$ to the hyperplane $\mathbf{a}_k^T\mathbf{x} = b_k$ for $k = 1, 2, \ldots, m$. For each iteration, $\mathbf{x}_{k+1}$ will convergent to the solution if the vectors $\mathbf{a}_1$, $\mathbf{a}_2$, …, $\mathbf{a}_m$ span $\mathbb{R}^n$. Therefore, in each iteration, we calculate the iterative vector:

$$\mathbf{x}_{k+1} = \mathbf{x}_k + \frac{\mathbf{b} - \mathbf{a}_k^T\mathbf{x}_k}{\mathbf{a}_k^T\mathbf{a}_k}\mathbf{a}_k$$

3. Test Problems

The rowaction ART is benchmarked using 4 cases, of which two cases are x-ray CT scan tests, a case from seismic tomography, and lastly a case of CT-scan of walnut.

3.1. Medical Imaging

Parallel beams tomography arise from medical sciences and used in medical imaging, X-ray CT scan geometries. We use parallel rays in some degrees to calculate the position and the interior of an object. This techniques also known as first generation, translate-rotate pencil beam geometry.

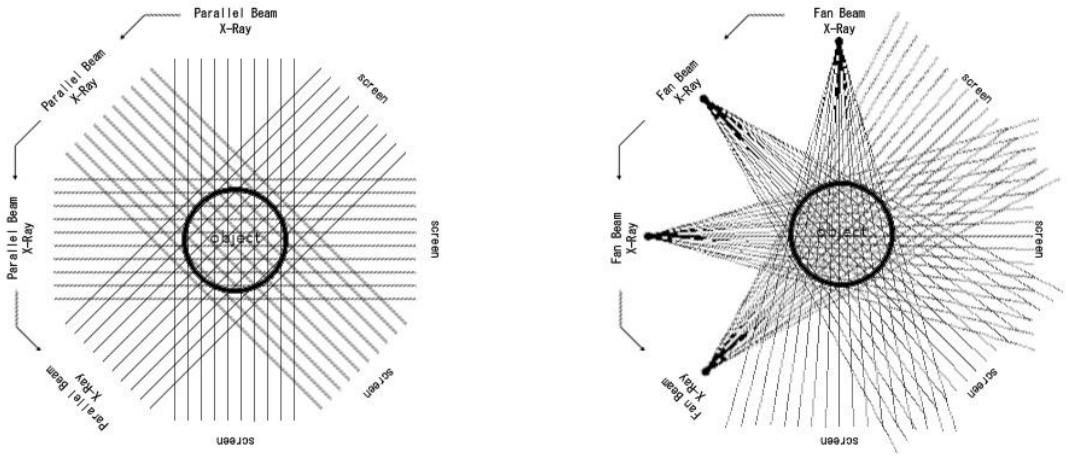

(**a**) (**b**)

Figure 1. Illustration of (a) Parallel Beams Tomography, (b) Fan Beams Tomography

Fan beams tomography also arise from medical sciences and used in medical imaging, X-ray CT scan geometries. In this techniques, we use point beam with fan-like forms rays through an object. These techniques also known as second generation, translate-rotate fan beam geometry.The object used in the experiment is modified Shepp Logan phantom with the discretization [3].

Preprints (www.preprints.org) | NOT PEER-REVIEWED | Posted: 5 June 2020 doi:10.20944/preprints202006.0053.v1

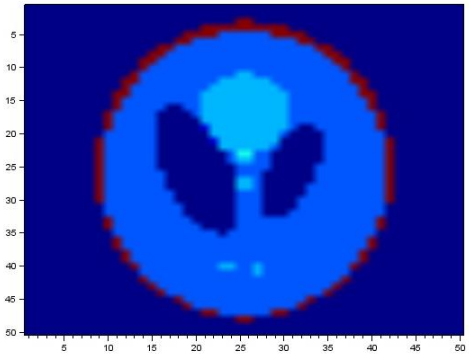

Figure 2. Illustration of Shepp Logan Phantom

Characteristics of matrix used in experiment is given in the Table 1.

Table 1. Medical Imaging Matrix Characteristics

	Parallel beams tomography	**Fan beams tomography**
Size of Coefficient Matrix	2700 × 2500	2700 × 2500
Number of nonzero elements in the Coefficient Matrix	114484(1.69%)	132604 (1.96%)
Maximum Value of Coefficient Matrix	1.1412	1.4142
Minimum Value of Coefficient Matrix	0.0002069	0.0001421
Maximum Value of RHS Vector	12.9894	13.8333
Minimum Value of RHS Vector	0.0004451	0.0004804

Both parallel beams and fan beams tomography coefficient matrix is based on *AIR Tools – A MATLAB package of algebraic iterative reconstruction methods* [1]. By multiplication ofthe desired coefficient matrix with modified Shepp Logan phantom, we obtain the RHS vector.

3.2. *Seismic Tomography*

Seismic tomography is a technique for imaging Earth subsurface characteristics. We placed the sources on the right side of the area and the receivers on the left side and the surface of the area.

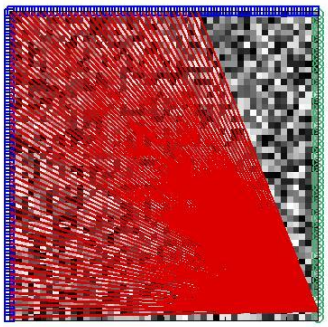

Figure 3. Illustration of Seismic Tomography

Seismic tomography is a technique for imaging Earth sub surface characteristics. The object used in the experiment is tectonic phantom with the discretization as in [3].

Preprints (www.preprints.org) | NOT PEER-REVIEWED | Posted: 5 June 2020 doi:10.20944/preprints202006.0053.v1

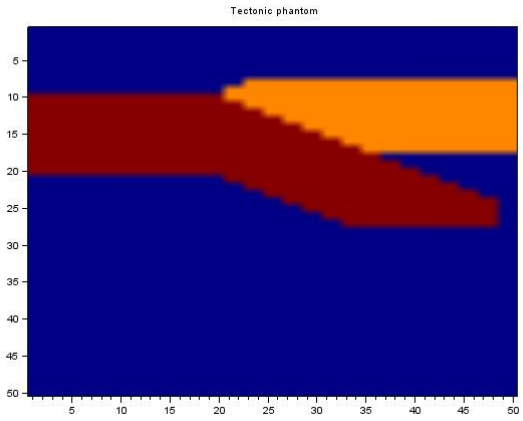

Figure 4. Illustration of tectonic phantom

Table 2 shows the characteristic of matrix used in the experiment.

Table 2. Seismic Tomography Matrix Characteristics

	Seismic Tomography
Size of Coefficient Matrix	5000 × 2500
Number of nonzero elements	288400 (2.31 %)
Maximum Value of Coefficient Matrix	1.4001
Minimum Value of Coefficient Matrix	0.0072
Maximum Value of RHS Vector	51.0157
Minimum Value of RHS Vector	0

3.3. Walnut Tomography

Tomographic X-ray data of a walnut taken from [4]. We use X-ray sinogram of a single 2D slice of the walnut of two different resolutions, $82 \times 82$and 164×164. Projections measured by 120 fan beams tomography of a walnut.

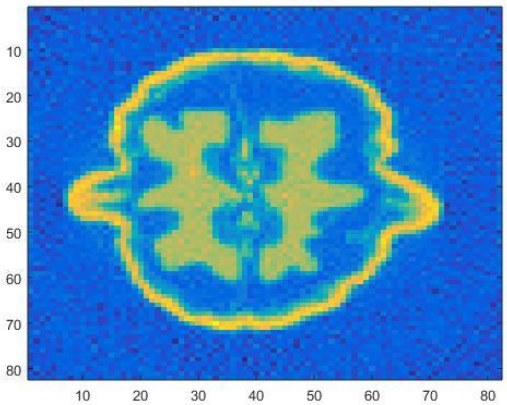

Figure 5. Illustration of walnut phantom

Characteristics of matrix used in experiment is given in the Table below.

Preprints (www.preprints.org) | NOT PEER-REVIEWED | Posted: 5 June 2020 doi:10.20944/preprints202006.0053.v1

Table 3. Walnut Matrix Characteristics

	Resolution 82 × 82	**Resolution 164 × 164**
Size of Coefficient Matrix	9840 × 6724	19680 × 26896
Number of nonzero elements in the Coefficient Matrix	970344 (1.47 %)	3881532 (0.73%)
Maximum Value of CoefficientMatrix	0.7234497	0.3625715
Minimum Value of Coefficient Matrix	0	0
Maximum Value of RHS Vector	0.9213660	0.9368123
Minimum Value of RHS Vector	0	0

4. Computational Result (Discussion)

All the computational experiment in this paper is conducted in the computer laboratory, Department of Mathematics, Faculty of Mathematics and Natural Sciences, Bogor Agricultural University. Computer specifications used are Processor Intel Core i5-3317U 1.7 GHz, RAM 4 GB, VGA NVIDIA GeForce GT 635M. The experiment was done in Microsoft Windows 7 using SCILAB 5.5.2 [https://www.scilab.org/download/5.5.2] with sciGPGPU 2.0 toolbox [https://atoms.scilab.org/toolboxes/sciGPGPU] for GPU support and plotlib 0.46 toolbox [https://atoms.scilab.org/toolboxes/plotlib/0.46] for graphing support.

Algebraic reconstruction techniques (ART) produces an iterative solution with given coefficient matrix and right hand side vector. We reproduce approximate solution with increased iteration numbers by using original coefficient matrix and right hand side vector. Both tomography techniques produces different results below.

Additionally, we test the problems by giving some perturbation to the right hand side vector in the form of random error vector. With an additional vector, we also reproduce approximate solution with increased iteration numbers.

$$\mathbf{b}_{new} = \mathbf{b} + \eta \frac{\|\mathbf{b}\|}{\|\boldsymbol{e}\|} \boldsymbol{e}$$

where $\boldsymbol{e}$is a random error vector and η is some small number (in this experiment we use $\eta = 0.05$).

4.1. Parallel Beams Tomography Result

In this subsection, we present the result for the parallel beams tomography for the original and perturbed RHS. Figures 6 — 9 show the approximation data represented by the scaled images using SCILAB's plotlib 0.46 toolbox [https://atoms.scilab.org/toolboxes/plotlib/0.46]for selected iterations (1, 10, 100 and 1000 iterations).

(**a**) (**b**)

Figure 6.1 ART iteration solver for parallel beams tomography (**a**) original right hand side; (**b**) perturbed right hand side.

Preprints (www.preprints.org) | NOT PEER-REVIEWED | Posted: 5 June 2020 doi:10.20944/preprints202006.0053.v1

(**a**) (**b**)

Figure 7.10 ART iterations solver for parallel beams tomography (**a**) original right hand side; (**b**) perturbed right hand side.

(**a**) (**b**)

Figure 8.100 ART iterations solver for parallel beams tomography (**a**) original right hand side; (**b**) perturbed right hand side.

(**a**) (**b**)

Figure 9.1000 ART iterations solver for parallel beams tomography (**a**) original right hand side; (**b**) perturbed right hand side.

By some observations, the more ART iterations performed, the approximation data represented by scaled images looksbetter than small ART iterations.Table 3 shows that the approximate solution is closer to exact solution, shown by smaller value of $\|A\boldsymbol{x}^* - \boldsymbol{b}\|$. On the other hand, the perturbed right hand side also give approximate solution that is closer to exact solution, shown by smaller value of $\|A\boldsymbol{x}^* - \boldsymbol{b}\|$, even with slower rate of convergence.

Table 4. Error rates for selected iterations

Number of iterations	Original RHS		Perturbed RHS	
	$\|Ax^* - b\|$	Time elapsed	$\|Ax^* - b_{new}\|$	Time elapsed
1 ART iteration	55.411	0.421s	57.605	0.437s
10 ART iterations	5.214	4.149s	16.202	4.181s
100 ART iterations	0.568	42.042s	15.013	44.741s
1000 ART iterations	0.212	436.97s	14.682	433.12s

Preprints (www.preprints.org) | NOT PEER-REVIEWED | Posted: 5 June 2020 doi:10.20944/preprints202006.0053.v1

The graphical view of the error rates forevery iterationsare shown in Figure 10.

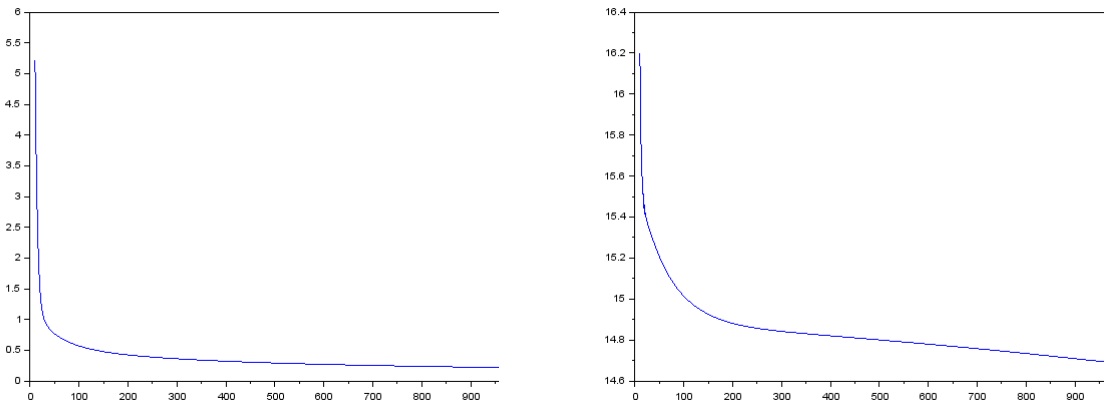

(**a**) (**b**)

Figure 10. Parallel beams tomography error rates for (**a**) original RHS and (**b**) perturbed RHS

As shown by the table and images, both cases converge to the exact solution as iteration increases, even though it converges to different values of norm because of perturbation that we have given above.

4.2. Fan Beams Tomography Result

In this subsection, we present the result for the fan beams tomography for the original and perturbed RHS. As in the previous subsection, Figures 11 – 14 show the approximation data represented by the scaled images using SCILAB's plotlib 0.46 toolbox [https://atoms.scilab.org/toolboxes/plotlib/0.46] for selected iterations (1, 10, 100 and 1000 iterations).

(**a**) (**b**)

Figure 11.1 ART iteration solver for fan beams tomography (**a**) original right hand side; (**b**) perturbed right hand side.

(**a**) (**b**)

Figure 12.10 ART iterations solver for fan beams tomography (**a**) original right hand side; (**b**) perturbed right hand side.

Preprints (www.preprints.org) | NOT PEER-REVIEWED | Posted: 5 June 2020 doi:10.20944/preprints202006.0053.v1

(**a**) (**b**)

Figure 13.100 ART iterations solver for fan beams tomography (**a**) original right hand side; (**b**) perturbed right hand side.

(**a**) (**b**)

Figure 14.1000 ART iterations solver for fan beams tomography (**a**) original right hand side; (**b**) perturbed right hand side.

By some observations, the more ART iterations performed, the approximation data represented by scaled images looksbetter than small ART iterations. Table 4 shows that the approximate solution is closer to exact solution, shown by smaller value of $\|A\boldsymbol{x}^* - \boldsymbol{b}\|$. On the other hand, the perturbed right hand side also give approximate solution that is closer to exact solution, shown by smaller value of $\|A\boldsymbol{x}^* - \boldsymbol{b}\|$, even with slower rate of convergence due to the perturbed condition.We can see that the fan beams tomography gives the similar result with parallel beams tomography.

Table 5. Error rates for selected iterations

Number of iterations	Original RHS		Perturbed RHS	
	$\|Ax^* - b\|$	Time elapsed	$\|Ax^* - b_{new}\|$	Time elapsed
1 ART iteration	60.242	0.499s	61.907	0.499s
10 ART iterations	3.556	4.836s	11.078	4.836s
100 ART iterations	0.785	48.75s	10.039	46.05s
1000 ART iterations	0.231	470.53s	8.929	481.49s

The graphical view of the error rates for every iterations give similar conclusion with parallel beams tomography as shown in Figure 15.

Preprints (www.preprints.org) | NOT PEER-REVIEWED | Posted: 5 June 2020 doi:10.20944/preprints202006.0053.v1

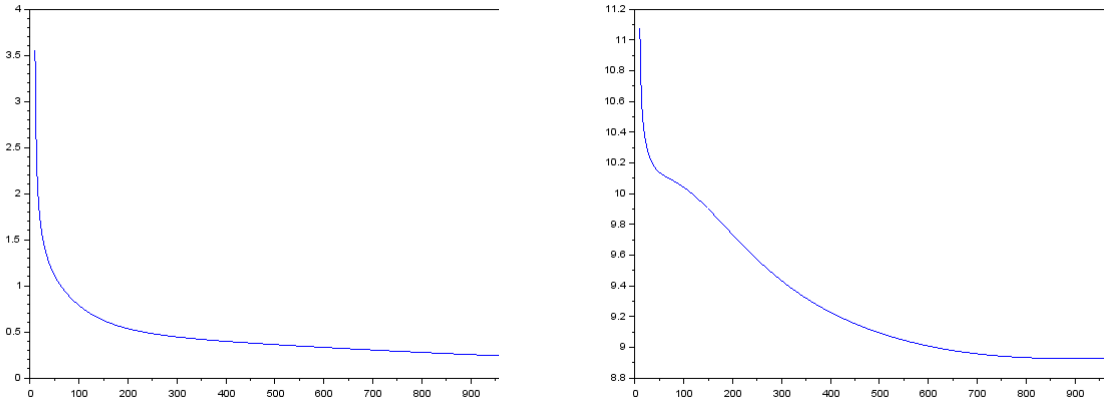

(**a**) (**b**)

Figure 15. Fan beams tomography error rates for (**a**) original RHS and (**b**) perturbed RHS

4.3. Seismic Tomography Result

In this subsection, we apply ART iterations for the seismic tomography data. Figures 16 – 19 show the approximation data represented by the scaled images using SCILAB's plotlib 0.46 toolbox [https://atoms.scilab.org/toolboxes/plotlib/0.46] for selected iterations (1, 10, 100 and 1000 iterations).

(**a**) (**b**)

Figure 16.1 ART iteration solver for seismic tomography (**a**) original right hand side; (**b**) perturbed right hand side.

(**a**) (**b**)

Figure 17.10 ART iterations solver for seismic tomography (**a**) original right hand side; (**b**) perturbed right hand side.

(**a**) (**b**)

Figure 18.100 ART iterations solver for seismic tomography (**a**) original right hand side; (**b**) perturbed right hand side.

Preprints (www.preprints.org) | NOT PEER-REVIEWED | Posted: 5 June 2020 doi:10.20944/preprints202006.0053.v1

(**a**) (**b**)

Figure 19.1000 ART iterations solver for seismic tomography (**a**) original right hand side; (**b**) perturbed right hand side.

The seismic tomography also gives us a similar conclusion: increased ART iterations converges better while perturbed images look worse than a smaller number of iterations. The error rates progression also agrees with both parallel beams and fan beams tomography as shown in Table 5 and Figure 20.

Table 6. Error rates for selected iterations

Number of iterations	Original RHS		Perturbed RHS	
	$\|Ax^* - b\|$	Time elapsed	$\|Ax^* - b_{new}\|$	Time elapsed
1 ART iteration	1002.028	0.608s	1016.642	0.749s
10 ART iterations	54.019	4.898s	97.599	3.744s
100 ART iterations	1.387	33.166s	79.016	37.331s
1000 ART iterations	0.1688	385.447s	77.796	386.243s

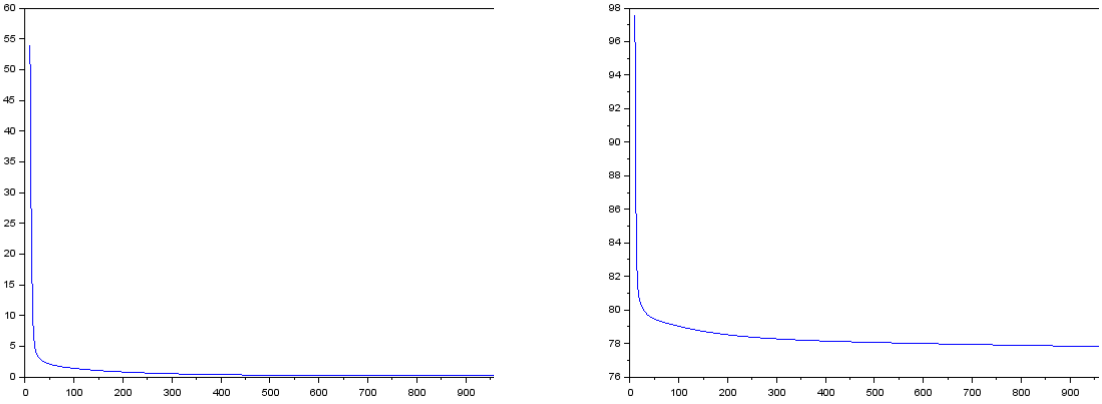

(**a**) (**b**)

Figure 20. Seismic tomography error rates for (**a**) original RHS and (**b**) perturbed RHS.

4.4. Walnut Tomography Result

In this subsection, we apply the ART iterations for the walnut tomography. The real walnut tomography data was capturedon 82 × 82 and 164 × 164resolutions.Figures 21 – 28 show the approximation data represented by the scaled images using SCILAB's plotlib 0.46 toolbox [https://atoms.scilab.org/toolboxes/plotlib/0.46] for selected iterations (1, 10, 100 and 1000 iterations).

Preprints (www.preprints.org) | NOT PEER-REVIEWED | Posted: 5 June 2020 doi:10.20944/preprints202006.0053.v1

4.4.1. Walnut with 82 × 82 resolutions

(**a**) (**b**)

Figure 21.1 ART iteration solver for walnut tomography (**a**) original right hand side; (**b**) perturbed right hand side.

(**a**) (**b**)

Figure 22.10 ART iterations solver for walnut tomography (**a**) original right hand side; (**b**) perturbed right hand side.

(**a**) (**b**)

Figure 23.100 ART iterations solver for walnut tomography (**a**) original right hand side; (**b**) perturbed right hand side.

(**a**) (**b**)

Figure 24.1000 ART iterations solver for walnut tomography (**a**) original right hand side; (**b**) perturbed right hand side.

Table 7. Error rates for selected iterations

Number of iterations	Original RHS		Perturbed RHS	
	$\|Ax^* - b\|$	Time elapsed	$\|Ax^* - b_{new}\|$	Time elapsed

Preprints (www.preprints.org) | NOT PEER-REVIEWED | Posted: 5 June 2020 doi:10.20944/preprints202006.0053.v1

1 ART iteration	10.160	0.9048s	10.443	0.920s
10 ART iterations	8.649	8.798s	8.604	8.720s
100 ART iterations	7.195	88.437s	7.306	87.283s
1000 ART iterations	6.736	881.468s	7.029	871.359s

4.4.2. Walnut with 164 × 164 resolutions

(**a**) (**b**)

Figure 25.1 ART iteration solver for walnut tomography (**a**) original right hand side; (**b**) perturbed right hand side.

(**a**) (**b**)

Figure 26.10 ART iterations solver for walnut tomography (**a**) original right hand side; (**b**) perturbed right hand side.

(**a**) (**b**)

Figure 27.100 ART iterations solver for walnut tomography (**a**) original right hand side; (**b**) perturbed right hand side.

(**a**) (**b**)

Figure 28.1000 ART iterations solver for walnut tomography (**a**) original right hand side; (**b**) perturbed right hand side.

Preprints (www.preprints.org) | NOT PEER-REVIEWED | Posted: 5 June 2020 doi:10.20944/preprints202006.0053.v1

Table 8. Error rates for selected iterations

Number of iterations	Original RHS		Perturbed RHS	
	$\|Ax^* - b\|$	Time elapsed	$\|Ax^* - b_{new}\|$	Time elapsed
1 ART iteration	14.346	6.942s	14.609	6.958s
10 ART iterations	11.745	68.531s	11.570	68.406s
100 ART iterations	3.789	685.188s	3.772	684.127s
1000 ART iterations	1.756	6841.705s	1.942	6907.849s

From Table 6 and 7, by adding ART iterations, all the approximate solutions are closer to the exact solutions, which can be seen in the scaled image. We can see that in the walnut tomography, the perturbed right-hand side still converges with similar rate as the original solution. This occurrence might be due to the right-hand side value range is minimal (from 0 to about 0.93) compared to the medical tomography (from 0 to about 13.83) and seismic tomography (from 0 to about 51.015). The graphical view of the error rates of every iterations for 164 × 164 resolution shown in Figure 29.The norms of the iteration also look very similar for82 × 82 resolution.

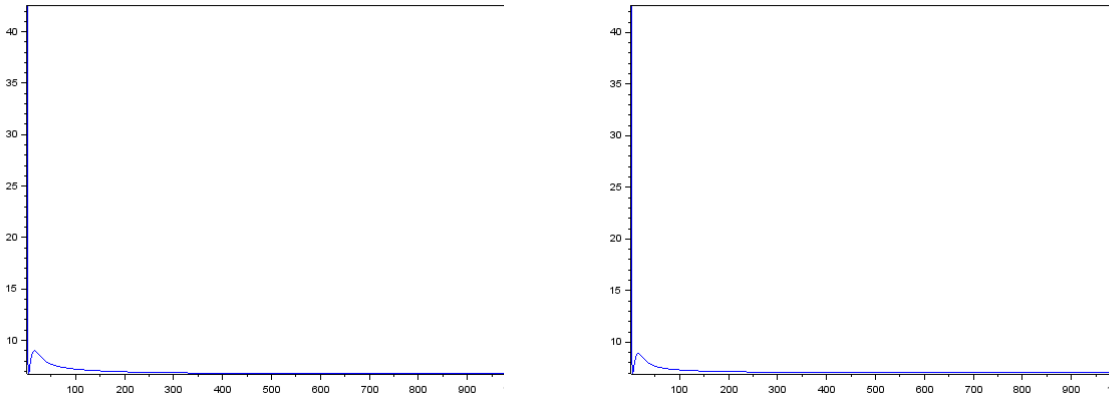

(**a**) (**b**)

Figure 29. Walnut tomography error rates for (**a**) original RHS and (**b**) perturbed RHS.

The left side images are ART iterations for walnut tomography with 82 × 82 resolution for the original problem, on the other hand, the right side images are ART iterations for the perturbed problem. As shown by images and small calculation, both problems converge and closer to the exact solution as iteration increased.

5. Conclusions

Both parallel beams tomography and fan beams tomography are widely used in CT scan geometries. This experiment shows that the parallelisation of algebraic reconstruction techniques to solve system of linear equations is successful. By adding more ART iterations, approximate solutions is closer to exact solution shown by smaller value of norm $\|Ax^* - b\|$, which is also matched with approximation data that represented by scaled image.

 doi:10.20944/preprints202006.0053.v1

With an additional error vector in hand right side vector, which we called perturbed systems, the approximate solution is harder to converge, again, shown by the value of norm $\|Ax^* - b\|$ even though time elapsed for solving the equation is not significantly different.

Since the perturbed vector is based on the magnitude of the right hand side, the walnut tomography – which has smallest maximum right hand side value – has the best approximation result for perturbed right hand side.

Author Contributions: Conceptualisation, ADG and SNI; methodology, ADG/MTJ/MIL; software, MIL; validation, ADG and MTJ; formal analysis, MTJ; resources, SNI; data curation, MIL; writing—original draft preparation, ADG/MIL/SNI; writing—review and editing, ADG/MIL; visualisation, MIL; supervision, SNI; project administration, ADG; funding acquisition, SNI. Author abbreviations: ADG, MIL, MTJ, SNI

Funding: This work was funded by the Ministry of Research and Higher Education, Republic of Indonesia, through the BOPTN Fiscal Year 2015, with contract no: 083/SP2H/PL/DitLitabmas/II/2015.

Conflicts of Interest: "The authors declare no conflict of interest."

References

1. Hansen, P.C.; Saxild-Hansen, M. AIR Tools – A MATLAB package of algebraic iterative reconstruction methods.*J. of Comp. App. Math.* **2012**,236, 2167-2178, https://doi.org/10.1016/j.cam.2011.09.039.
2. Kaczmarz, S. Angenäherte Auflösung von Systemen linearer Gleichungen, *Bulletin de l'Acad´ emie Polonaise des Sciences et Lettres*, **1937**, A35, pp. 355–357.
3. Kak, A. C.; Slaney,M.; *Principles of Computerized Tomographic Imaging*; SIAM: Philadelphia, USA,2001;ISBN.978-08987149
4. Hämäläinen, K.; Harhanen, L.; Kallonen, A.; Kujanpää, A.;Niemi, E.; Siltanen, S. Tomographic X-ray data of a walnut. *Preprint arXiv*, **2015**,arXiv: 1502.04064v1 [physics.data-an]
5. Hansen, P.C.; Jørgensen, J.S. "AIR Tools II: algebraic iterative reconstruction methods, improved implementation. *Numer.Algo.* , **2018**, 79, no. 1, 107-137,http://dx.doi.org/10.1007/s11075-017-0430-x